



How skillfully can we simulate drivers of aerosol direct climate forcing at the regional scale?

P. Crippa et al.

How skillfully can we simulate drivers of aerosol direct climate forcing at the regional scale?

P. Crippa¹, R. C. Sullivan², A. Thota³, and S. C. Pryor^{2,3}

¹COMET, School of Civil Engineering and Geosciences, Cassie Building, Newcastle University, Newcastle upon Tyne, NE1 7RU, UK

²Department of Earth and Atmospheric Sciences, Bradfield Hall, 306 Tower Road, Cornell University, Ithaca, NY 14853, USA

³Pervasive Technology Institute, Indiana University, Bloomington, IN 47405, USA

Received: 29 July 2015 – Accepted: 19 September 2015 – Published: 8 October 2015

Correspondence to: P. Crippa (paola.crippa@ncl.ac.uk)

Published by Copernicus Publications on behalf of the European Geosciences Union.

Title Page

Abstract

Introduction

Conclusions

References

Tables

Figures



Back

Close

Full Screen / Esc

Printer-friendly Version

Interactive Discussion



Abstract

Assessing the ability of global and regional models to describe aerosol optical properties is essential to reducing uncertainty in aerosol direct radiative forcing in the contemporary climate and to improving confidence in future projections. Here we evaluate the skill of high-resolution simulations conducted using the Weather Research and Forecasting model with coupled chemistry (WRF-Chem) in capturing spatio-temporal variability of aerosol optical depth (AOD) and Ångström exponent (AE) by comparison with ground- and space- based remotely sensed observations. WRF-Chem is run over eastern North America at a resolution of 12 km for a representative year (2008). A small systematic positive bias in simulated AOD relative to observations is found (annual MFB = 0.17 and 0.50 when comparing with MODIS and AERONET respectively), whereas the spatial variability is well captured during most months. The spatial correlation of AOD shows a clear seasonal cycle with highest correlation during summer months ($r = 0.5\text{--}0.7$) when the aerosol loading is large and more observations are available. AE is retrieved with higher uncertainty from the remote sensing observations. The model is biased towards simulation of coarse mode aerosols (annual MFB for AE = -0.10 relative to MODIS and -0.59 for AERONET), but the spatial correlation for AE with observations is $0.3\text{--}0.5$ during most months. WRF-Chem also exhibits high skill in identifying areas of extreme and non-extreme aerosol loading, and its ability to correctly simulate the location and relative intensity of an extreme aerosol event (i.e. AOD > 75th percentile) varies between 30 and 70 % during winter and summer months respectively.

1 Introduction and objectives

Atmospheric aerosol particles (aerosols) play a major role in dictating Earth's climate by both directly interacting with solar radiation (direct effect) and acting as cloud condensation nuclei and thus changing cloud properties (indirect effect) (Boucher et al.,

ACPD

15, 27311–27355, 2015

How skillfully can we simulate drivers of aerosol direct climate forcing at the regional scale?

P. Crippa et al.

Title Page

Abstract

Introduction

Conclusions

References

Tables

Figures

◀

▶

◀

▶

Back

Close

Full Screen / Esc

Printer-friendly Version

Interactive Discussion



2013). The global mean aerosol direct effect is estimated to be -0.27 (possible range of -0.77 to $+0.23$) $W m^{-2}$, while the indirect effect is -0.55 (-1.33 to -0.06) $W m^{-2}$ (Stocker et al., 2013). Therefore their combined radiative forcing is likely a significant fraction of the overall net anthropogenic climate forcing since pre-industrial times (i.e. 1.13–3.33 $W m^{-2}$, Stocker et al., 2013) and a substantial source of uncertainty in quantifying anthropogenic radiative forcing.

Accurate quantification of direct aerosol radiative forcing is strongly dependent on aerosol precursor and primary aerosol emissions. Both have evolved over the past two decades in terms of their spatio-temporal distribution and absolute magnitude. Emissions have generally increased in emerging economies (Kurokawa et al., 2013), biogenic and anthropogenic emissions have altered in response to changing land use and land cover (Wu et al., 2012), and the implementation of pollution control strategies particularly in North America and Europe have resulted in declines in air pollutant emissions (Xing et al., 2015; Giannouli et al., 2011). Therefore there is evidence that aerosol burdens and thus direct climate forcing has varied markedly in the past and may change substantially in the future. Further, although best estimates of global anthropogenic radiative forcing from the aerosol direct and indirect effect are -0.27 and -0.55 $W m^{-2}$ (Stocker et al., 2013) respectively, the short residence time and high spatio-temporal variability of aerosol populations mean their impact on regional climates can be much larger than the global mean but are even more uncertain.

Long-term continuous and high precision measurements of aerosol properties are largely confined to aerosol mass (total, PM_{10} or $PM_{2.5}$) in the near-surface layer which may or may not be representative of either the total atmospheric burden (Ford and Heald, 2013; Alston et al., 2012), or radiation extinction and hence climate forcing. Columnar remote sensing measurements of aerosol optical properties are available from a range of ground-based and satellite-borne instrumentation, but have only a relatively short period of record, are subject to non-zero measurement uncertainty (and bias), and under-sample the range of atmospheric conditions due to cloud masking and infrequent satellite overpasses. Therefore, regional and global models are most

How skillfully can we simulate drivers of aerosol direct climate forcing at the regional scale?

P. Crippa et al.

[Title Page](#)[Abstract](#)[Introduction](#)[Conclusions](#)[References](#)[Tables](#)[Figures](#)[◀](#)[▶](#)[◀](#)[▶](#)[Back](#)[Close](#)[Full Screen / Esc](#)[Printer-friendly Version](#)[Interactive Discussion](#)

commonly used to quantify historical and contemporary aerosol direct radiative forcing based on simulated properties such as the aerosol optical depth (AOD) and Ångström exponent (AE) (Boucher et al., 2013).

Most global models that include aerosol microphysics have been run at fairly coarse resolution (spatial resolution of the order of 1–2.5°) (Table 1) usually for periods of a few years. The resulting fields of AOD (and less frequently AE) have been evaluated relative to ground-based and satellite-borne remote sensing optical properties measurements (Table 1). However, aerosol populations (and dynamics) are known to exhibit higher spatial variability (and scales) than can be manifest in those models (Kulmala et al., 2011; Spracklen et al., 2010). Despite recent improvements in the sophistication of aerosol processes and properties within global models, there are still substantial regional and latitudinal discrepancies in both the magnitude of AOD and other aerosol properties which impact aerosol direct radiative forcing and the degree of model-to-model agreement (Myhre et al., 2013). The skill of these models in reproducing the spatio-temporal variability in the aerosol size distribution, composition, concentration and radiative properties is incompletely characterized. Accordingly, there is large model-to-model variability both in the global mean direct aerosol forcing and in the spatial distribution thereof (Kulmala et al., 2011; Myhre et al., 2013). Although a direct comparison between the studies summarized in Table 1 is inherently very difficult due to the different performance metrics reported, and variations in both the model resolution and aerosol descriptions, there is a consistent finding of high spatial variability in model bias, both in sign and magnitude. Correlation coefficients of monthly and seasonal mean AOD from model simulations vs. satellite-based measurements are typically in a range ~ 0.6 – 0.8 both in global (Colarco et al., 2010; Lee et al., 2015) and regional (Nabat et al., 2015) simulations. However, these correlations are largely reflective of the ability of the models to capture the seasonal cycle and columnar aerosol properties from remote sensing and thus ignore substantial variability on the synoptic (Sullivan et al., 2015) and meso-scales (Anderson et al., 2003). A wider range of correlation coefficients are reported when comparisons are made to high fre-

How skillfully can we simulate drivers of aerosol direct climate forcing at the regional scale?

P. Crippa et al.

Title Page

Abstract

Introduction

Conclusions

References

Tables

Figures

◀

▶

◀

▶

Back

Close

Full Screen / Esc

Printer-friendly Version

Interactive Discussion



How skillfully can we simulate drivers of aerosol direct climate forcing at the regional scale?

P. Crippa et al.

Title Page

Abstract

Introduction

Conclusions

References

Tables

Figures

◀

▶

◀

▶

Back

Close

Full Screen / Esc

Printer-friendly Version

Interactive Discussion

quency observations of AOD at the hourly/daily timescale both in global (Sič et al., 2015) and regional (Rea et al., 2015) simulations ($r \sim 0.3$ – 0.8). The largest range of correlation coefficients ($[-0.99, 0.9]$; Table 1) is reported when simulated AOD is compared with observations from the AErosol RObotic NETwork (AERONET), and appear to be function of temporal averaging, location of AERONET sites and model resolution. Correlations between time series of simulated AE vs. AERONET observations are reported less frequently, and when conducted for monthly mean values range from ~ 0.4 (Li et al., 2015) to ~ 0.8 (Colarco et al., 2010).

At least some of the variability in model skill, as indicated by the mutual variability with observations described by correlation coefficients, and model-to-model agreement shown in AeroCom Phase II may be attributable to variations in model resolution, differences in gas and particle phase parameterizations and aerosol descriptions. However, there are also variations in the way in which model skill is evaluated leading to ambiguity in terms of prioritizing future research directions. The direct effect remains poorly quantified at the regional scale, due to uncertainty in aerosol loading, uncertainty and spatio-temporal variability in aerosol physical properties (Colarco et al., 2014) and a relative paucity of rigorous model verification and validation exercises. Confidence in projections of possible future aerosol radiative forcing requires detailed assessment of skill in the current climate, and the need for and benefits of regional downscaling and/or use of high-resolution global models requires careful quantification.

Regional models represent an opportunity to assess if running higher resolution simulations over specific regions of interest improves the characterization of aerosol optical properties of relevance to direct radiative forcing. Assessment of value added (or lack thereof) from high resolution regional vs. global coarse resolution models is not quantifiable from prior studies alone. Although high-resolution simulations, comparable to those presented herein, have been run, they are over a small temporal and spatial domain (e.g., Tuccella et al., 2015), or lack quantitative assessment of aerosol optical properties (e.g., Tessum et al., 2014). Thus, quantification of the skill of high-resolution modeling of aerosol optical properties is presented here. Forthcoming work will include

direct comparison to coarser resolution simulations to quantify the value added (or lack thereof) from increased model resolution.

We evaluate the skill of state-of-the-art high-resolution regional model simulations of climate-relevant aerosol properties using a range of inferential statistics and investigate possible sources of discrepancies with observations. The impact of aerosols on climate and human health are strengthened under conditions of enhanced aerosol concentrations, thus it is necessary to study and diagnose causes of “extreme aerosol events” (Chu, 2004; Gkikas et al., 2012), and to evaluate the ability of numerical models to simulate their occurrence, intensity, spatial extent and location. Prior analyses of Level-3 (1° resolution) MODIS AOD over the eastern half of North America have indicated the frequency of co-occurrence of extreme AOD values (> local 90th percentile) decreases to below 50% at ~ 150 km from a central grid cell located in southern Indiana, but is above that expected by random chance over almost all of eastern North America (Sullivan et al., 2015). Thus, our evaluation exercise also includes an analysis of the spatio-temporal coherence of extreme events.

We applied the Weather Research and Forecasting model with coupled Chemistry (WRF-Chem version 3.6.1) at high resolution (12 × 12 km) over eastern North America during the year 2008, in the context of a pseudo type-2 downscaling exercise in which the high-resolution model is nested within reanalysis boundary conditions (Castro et al., 2005). The choice of this spatial resolution is taken in part to match the resolution of North American Mesoscale Model that is used for the meteorological lateral boundary conditions and to ensure we capture some mesoscale variability while remaining computationally feasible.

Our evaluation is designed to investigate spatio-temporal variability of aerosol optical properties (i.e. AOD and AE) in their mean and extreme values. Thus, we conduct our evaluation of the simulations using:

1. High-frequency, disjunct time series data from columnar point measurements at AERONET stations.

How skillfully can we simulate drivers of aerosol direct climate forcing at the regional scale?

P. Crippa et al.

Title Page	
Abstract	Introduction
Conclusions	References
Tables	Figures
◀	▶
◀	▶
Back	Close
Full Screen / Esc	
Printer-friendly Version	
Interactive Discussion	



2. Relatively high-resolution spatial data from lower frequency (once daily or lower) data from polar orbiting satellites (i.e. MODIS and MISR).

We also include intercomparison with daily mean $PM_{2.5}$ concentrations from 1230 surface stations. These data for 2008 were obtained from the US Environmental Protection Agency (EPA) AirData web site and represent all available outdoor near-surface 24 h mean $PM_{2.5}$ measurements in the model domain. Most of these stations report values on a 1 day in 3 schedule. We further evaluate the WRF-Chem simulations of a key meteorological parameter – precipitation – relative to observations from the Delaware gridded dataset (Matsuura and Willmott, 2009). This data set includes monthly accumulated precipitation data on a $0.5 \times 0.5^\circ$ grid which is estimated by interpolating station observations from the Global Historical Climatology Network using the spherical version of Shepard's distance-weighting method (Shepard, 1968; Willmott et al., 1985).

2 Methods

2.1 WRF-Chem simulations

The Weather Research and Forecasting Model with coupled chemistry (WRF-Chem, version 3.6.1) (Grell et al., 2005; Fast et al., 2006) is used to simulate aerosol processes over eastern North America during the whole of 2008. The simulation domain comprises 300×300 grid points with 12 km resolution and is centered in southern Indiana (86° W, 39° N). The calendar year 2008 was selected because it is representative of average climate and aerosol conditions in the center of the model domain (near Indianapolis, IN). In 2008, mean T_{\max} , T_{\min} , precipitation, and wind speed as measured at the National Weather Service Automated Surface Observing Systems (NWS ASOS) station at Indianapolis International Airport are within ± 0.25 standard deviations (σ) of the 2000–2013 seasonal means. Further, mean seasonal AOD from Level-3 MODIS retrievals is within $\pm 0.2\sigma$ of 2000–2013 mean values. Additionally, choice of this year

How skillfully can we simulate drivers of aerosol direct climate forcing at the regional scale?

P. Crippa et al.

Title Page

Abstract

Introduction

Conclusions

References

Tables

Figures

◀

▶

◀

▶

Back

Close

Full Screen / Esc

Printer-friendly Version

Interactive Discussion



ensures availability of multiple sources of ground- and space-based measurements of aerosol properties for evaluation of the simulations.

Table 2 provides details of the WRF-Chem simulations. In brief, we used 32 vertical levels up to 50 hPa with telescoping to allow for a good vertical resolution in the boundary layer (i.e. approximately 10 layers below 1 km for non-mountainous regions). Meteorological lateral boundary conditions are provided every 6 h from the North American Mesoscale Model (NAM) applied at 12 km resolution. The initial and boundary chemical conditions are based on output from the offline global chemical transport model MOZART-4 (Model for Ozone and Related chemical Tracers, version 4), driven by meteorology from NCEP/NCAR-reanalysis (Pfister et al., 2011; Emmons et al., 2010). Anthropogenic emissions are from the POET (Precursors of Ozone and their Effects in the Troposphere) and the EDGAR (Emissions Database for Global Atmospheric Research) databases. The land cover is specified based on the USGS 24-category data at 3.7 km resolution (Anderson et al., 1976). Anthropogenic point and area emissions at 4 km resolution are input hourly from the US National Emissions Inventory (NEI-05) (US-EPA, 2009) and specified for 19 vertical levels (see Fig. 1 for an overview of the primary aerosol emissions). Biogenic emissions of isoprene, monoterpenes, other biogenic VOC (OVOC), and nitrogen gas emissions from the soil are described as a function of simulated temperature and photosynthetic active radiation (for isoprene) using the model of Guenther (Guenther et al., 1993, 1994; Simpson et al., 1995). Aerosol and gas phase chemistry are described using the second generation Regional Acid Deposition Model (RADM2) chemical mechanism (Stockwell et al., 1990) and the Modal Aerosol Dynamics Model for Europe (MADE) which incorporates the Secondary Organic Aerosol Model (SORGAM) (Ackermann et al., 1998; Schell et al., 2001). The correct characterization of aerosol optical properties is strongly related to model skill in describing particle composition and mixing state (Li et al., 2015; Curci et al., 2014). With this in mind, it is worthy of note that aerosol components are assumed to be internally mixed within each mode (although the composition differs by mode). For the Aitken and accumulation modes the median diameters are 10 and 70 nm with standard

How skillfully can we simulate drivers of aerosol direct climate forcing at the regional scale?

P. Crippa et al.

Title Page

Abstract

Introduction

Conclusions

References

Tables

Figures

◀

▶

◀

▶

Back

Close

Full Screen / Esc

Printer-friendly Version

Interactive Discussion



deviations of 1.6 and 2, respectively. The choice of a modal representation of aerosol size distribution is dictated by the high computational demand of more sophisticated approaches (e.g. sectional description of the aerosol size distribution) for long-term simulations. With the current settings, the 1 year run was completed without restart in 9.5 days (230 h) on the Cray XE6/XK7 supercomputer (Big Red II) owned by Indiana University using 256 processors distributed on 8 nodes, thus indicating feasibility of this configuration for climate scale simulations. Aerosol, and gas phase concentrations and meteorological properties are saved once hourly. AE from the WRF-Chem simulations is computed using:

$$AE = \frac{\ln \frac{AOD_{400 \text{ nm}}}{AOD_{600 \text{ nm}}}}{\ln \frac{600 \text{ nm}}{400 \text{ nm}}} \quad (1)$$

AOD at wavelengths (λ) of 500 and 550 nm, for comparison with MODIS and MISR respectively, are derived using the Ångström power law:

$$AOD_{\lambda} = AOD_{300} \times \frac{\lambda}{300}^{(-AE)} \quad (2)$$

We investigated the wavelength dependence on AE calculation using λ at 300 and 1000 nm as proposed in (Kumar et al., 2014) and found that, although AOD estimates are independent on the wavelength range selected, $AE_{400-600 \text{ nm}}$ is systematically lower than $AE_{300-1000 \text{ nm}}$. Analyses of AE reported in this study are obtained using wavelengths at 400 and 600 nm since they are closer to those used in AE satellite retrievals.

2.2 Remotely-sensed data

Consistent with previous research (Sect. 1 and Table 1), we evaluate the WRF-Chem simulations using four primary remote sensing products – three are drawn from instruments on the Aqua and Terra satellites, while the fourth is from ground-based radiometers operated as part of the AERONET network. The data sets are as follows:

How skillfully can we simulate drivers of aerosol direct climate forcing at the regional scale?

P. Crippa et al.

Title Page

Abstract

Introduction

Conclusions

References

Tables

Figures

◀

▶

◀

▶

Back

Close

Full Screen / Esc

Printer-friendly Version

Interactive Discussion



How skillfully can we simulate drivers of aerosol direct climate forcing at the regional scale?

P. Crippa et al.

Title Page

Abstract

Introduction

Conclusions

References

Tables

Figures

◀

▶

◀

▶

Back

Close

Full Screen / Esc

Printer-friendly Version

Interactive Discussion

1. The MODerate resolution Imaging Spectroradiometer (MODIS) instruments aboard the polar-orbiting Terra (~ 10:30 overpass local solar time, LST) and Aqua (~ 13:30 LST) satellites. They have measured atmospheric aerosol optical properties since 2000 and 2002 respectively, with near-global daily coverage (Remer et al., 2005). Herein we use the Level 2 (L2; 10 km resolution) “dark-target” products of AOD at 550 nm and AE from 470–660 nm (Collection 5.1; Levy et al., 2010). The L2 AOD uncertainty is $\pm 0.05 \pm 0.15 \times$ AOD over land relative to global sun photometer measurements from AERONET. AE is retrieved with higher uncertainty, and tends to exhibit a bi-modality in retrieved values (Levy et al., 2010; Remer et al., 2005) (see Fig. S1 in the Supplement). For this reason where we compare WRF-Chem simulated AE with values from MODIS we treat AE as a binary variable, wherein $AE < 1$ is taken as representing coarse mode dominated aerosol populations and $AE > 1$ indicates fine mode dominated populations (Pereira et al., 2011; Valenzuela et al., 2014).
2. The Multi-angle Imaging Spectroradiometer (MISR) instrument is also aboard the Terra satellite, and measures radiances at four wavelengths from 446–886 nm at nine viewing angles from nadir to 70.5°. MISR (L2, 17.6 km resolution) retrieves AOD with lower uncertainty than MODIS ($\pm 0.05 \times$ AOD relative to AERONET), but with lower temporal resolution (global coverage in ~ one week) (Kahn et al., 2010, 2005). Herein, we use the $0.5^\circ \times 0.5^\circ$ gridded Level 3 (Ver. 31) AOD (at 555 nm) and AE (calculated from AOD at 443 and 670 nm).
3. Ground-based sun-photometer measurements from 22 AERosol RObotic NETwork (AERONET) (Holben et al., 1998) stations are also used in this study (Fig. 1). This network is highly spatially inhomogeneous, but under cloud-free conditions the observations are available at multiple times during daylight hours. AOD is measured directly by the AERONET sun photometers at seven wavelengths (340, 380, 440, 500, 670, 870, and 1020 nm) with high accuracy (i.e. AOD uncertainty of < 0.01 for $\lambda > 440$ nm, Holben et al., 2001). The Ångström Exponent (AE) is cal-

How skillfully can we simulate drivers of aerosol direct climate forcing at the regional scale?

P. Crippa et al.

Title Page

Abstract

Introduction

Conclusions

References

Tables

Figures

◀

▶

◀

▶

Back

Close

Full Screen / Esc

Printer-friendly Version

Interactive Discussion



culated for all available wavelengths within the AOD range. The AE 870–440 nm includes the 870, 670, 500 and 440 nm AOD data. Level-2 aerosol products from AERONET (i.e. cloud screened and quality assured) have been used extensively in satellite and model validation studies (including many of those summarized in Table 1) and are used herein.

To avoid the discontinuity in the MODIS retrieval algorithm due to different assumed aerosol types (Levy et al., 2007), we confine our analyses of model skill to longitudes east of 98° W. All comparisons of modeled aerosol optical properties relative to MODIS observations (e.g. monthly mean values) only include grid cells for which at least 5 valid coincident observations are available during a given month after applying a cloud screen for overpass hours with cloud fraction larger than zero. It is worth noting that setting a threshold of 10 observations does not significantly affect the results. For a uniform assessment, L2 MODIS and L3 MISR data have been interpolated from their native grids (and resolutions of 10 km and 0.5° × 0.5°, respectively) to the WRF-Chem 12 km resolution grid by computing the mean of pixels with valid data within 0.1° (~ 20 km) from the model centroids. The choice of averaging over a slightly larger area than model resolution is dictated by the sparsity of valid MODIS retrievals. Where WRF-Chem output is compared with data from AERONET stations, a station is only included if there are at least 20 simultaneous estimates available.

2.3 Statistical methods used in the model evaluation

The primary error metric of overall model performance used herein is the Mean Fractional Bias (Boylan and Russell, 2006):

$$\text{MFB} = \frac{1}{N} \sum_1^N \frac{C_m - C_0}{\frac{C_m + C_0}{2}}. \quad (3)$$

MFB is a useful model performance indicator since it equally weights positive and negative biases. It varies between +2 and –2 and has a value of zero for an ideal model.

How skillfully can we simulate drivers of aerosol direct climate forcing at the regional scale?

P. Crippa et al.

Title Page

Abstract

Introduction

Conclusions

References

Tables

Figures

◀

▶

◀

▶

Back

Close

Full Screen / Esc

Printer-friendly Version

Interactive Discussion

Where MFB is reported for WRF-Chem vs. MODIS or MISR, C_m is the monthly mean AOD or AE simulated by WRF-Chem at a specific location, C_0 refers to the same quantity from MODIS or MISR (Table 3) and N is the sample size. Where MFB is reported in comparisons of WRF-Chem with AERONET, the monthly average in the model grid cell containing the AERONET site is compared with monthly averaged observations (C_0).

The evaluation of WRF-Chem simulations of AOD and AE relative to satellite retrievals (MODIS and MISR) is also summarized using Taylor diagrams (Taylor, 2001) produced from the monthly means for the grid cells with simultaneous data availability. Taylor diagrams synthesize three aspects of model skill focused on evaluations of the spatial fields of the parameter of interest. The correlation coefficient of the modeled vs. observed field which is expressed by the azimuthal position, the root mean squared difference which is proportional to the distance between a point and the reference point on the x axis (at 1, 0), and the ratio of simulated and observed spatial standard deviation which is proportional to the radial distance from the origin.

To investigate model performance at given locations through time, empirical quantile-quantile (EQQ) plots are constructed using high frequency realizations of AOD and AE at individual locations (AERONET sites) relative to WRF-Chem values simulated in the grid cell containing the measurement site. EQQ plots are thus generated for each of the AERONET stations using all hours when there are simultaneous estimates available from the direct observations and from the numerical simulations. The advantage of EQQ plots is that they make no assumptions regarding the underlying form of the data, and can be readily used to determine which parts of the modeled distribution deviate from the observations (and thus fall away from a 1 : 1 line).

The validity of AE estimates is a function of both the absolute magnitude of AOD and the uncertainty in the wavelength dependent AOD. AE provides information regarding the relative abundance of fine to coarse particles. Thus, here we quantify the model skill in reproducing spatial patterns of fine and coarse mode particles observed by MODIS (Terra) by comparing the frequency distribution of AE lower and higher than 1 to distinguish populations dominated by coarse and fine aerosols respectively in WRF-

in WRF-Chem (WE) or MODIS (ME) or not (WN or MN):

$$\text{Accuracy} = \frac{\text{WE}/\text{ME} + \text{WN}/\text{MN}}{\text{WE}/\text{ME} + \text{WE}/\text{MN} + \text{WN}/\text{ME} + \text{WN}/\text{MN}} \quad (5)$$

$$\text{HR} = \frac{\text{WE}/\text{ME}}{\text{WE}/\text{ME} + \text{WN}/\text{ME}} \quad (6)$$

$$\text{TS} = \frac{\text{WE}/\text{ME}}{\text{WE}/\text{ME} + \text{WE}/\text{MN} + \text{WN}/\text{ME}} \quad (7)$$

The Accuracy describes the fraction of grid cells co-identified as exceeding p75 or not in MODIS and WRF-Chem, and thus equally weights event and non-event conditions. In this application, where extreme is identified as the 75th percentile, a value of 0.5 would indicate none of the grid cells experiencing extreme events were reproduced by the model, while 1 would indicate perfect identification of events and non-events. The HR and TS metrics give “credit” only those grid cells identified as “extreme”. For these metrics, a value of 0 indicates no correct identification of grid cells with extreme values, while a perfect model would exhibit a value of 1.

- Evaluation of the scales of coherence of extreme AOD. For each day during the overpass time and hours of clear sky conditions, we determine if AOD simulated at our reference location (i.e. the center of the domain, in Southern Indiana) is equal or larger than the local p75 for that grid cell and season and then identify all grid cells in the domain that also satisfy the condition of $\text{AOD} \geq \text{local p75}$. For each season, we thus compute the probability of extreme AOD co-occurrence at our reference site and any other grid cell as the frequency of co-occurrence divided by the number of extreme occurrences at the reference location. The spatial scales of extreme AOD are then estimated by binning the radial distance of each grid cell centroid from the domain center into 100 km distance classes. An analogous procedure is applied to L2 MODIS data to compare with simulations.

27324

How skillfully can we simulate drivers of aerosol direct climate forcing at the regional scale?

P. Crippa et al.

Title Page

Abstract

Introduction

Conclusions

References

Tables

Figures



Back

Close

Full Screen / Esc

Printer-friendly Version

Interactive Discussion



3 Results

3.1 Evaluation of AOD

Overall WRF-Chem is positively biased relative to remotely-sensed AOD. The spatial MFB is 0.20 (0.14) when computed using all available MODIS measurements from Terra (Aqua) and 0.50 relative to data from the AERONET stations (Table 3). The sign of this bias is consistent across the entire simulation domain (Fig. 2). These results agree with findings from previous regional studies that have also shown an overestimation of AOD by WRF-Chem over eastern North America and Europe (i.e. regions dominated by sulfate aerosols), and underestimation in western US and most of the rest of the globe (Zhang et al., 2012; Colarco et al., 2010; Curci et al., 2014) (Table 1). Higher biases of WRF-Chem simulated annual mean AOD are found in the southern portion of the domain (Fig. 2) where the model also exhibits a positive bias in daily mean near-surface PM_{2.5} relative to observations from 1230 US EPA sites (see Fig. 3 and Fig. S2). The MFB of WRF-Chem relative to MODIS estimates of AOD is lower than the MFB relative to most of the AERONET stations except for a few sites located along the coast, one polluted site in the northeast and a few land sites in the North/North-West (Fig. 2c and 4a). This is possibly a result of an inability of the model to capture variations in aerosol optical properties occurring at a local scale (below the resolution of 12 km). However, the evaluation statistics for WRF-Chem relative to AERONET did not vary consistently with the classification of AERONET stations. Indeed, the mean MFB for AOD in coastal, polluted and land sites varies between 0.26 (coastal) and 0.67 (land), whereas for AE it varies between -0.72 (coastal) and -0.50 (land).

Spatial patterns of monthly mean AOD show largest differences relative to MODIS during winter months in the southern states and near the coastlines, which show MFB up to 0.7, and lower spatial correlation (see Fig. 5a). This may be due to the larger uncertainty in MODIS retrievals near the coast (Anderson et al., 2013), the smaller sample size in the observations (particularly at high latitudes) during December to March or the lower overall AOD. Conversely, the spatial correlation is maximized over the summer

How skillfully can we simulate drivers of aerosol direct climate forcing at the regional scale?

P. Crippa et al.

Title Page

Abstract

Introduction

Conclusions

References

Tables

Figures



Back

Close

Full Screen / Esc

Printer-friendly Version

Interactive Discussion



How skillfully can we simulate drivers of aerosol direct climate forcing at the regional scale?

P. Crippa et al.

Title Page

Abstract

Introduction

Conclusions

References

Tables

Figures

◀

▶

◀

▶

Back

Close

Full Screen / Esc

Printer-friendly Version

Interactive Discussion



($r = 0.5$ – 0.7) for MODIS and August for MISR, when most data are available. The spatial variability of monthly mean AOD fields is also well simulated by WRF-Chem during the warm season (months May–August), as indicated by the ratio of the spatial standard deviation is close to 1. However, it is usually higher in MODIS and/or MISR than in WRF-Chem. The RMSD is largest and the spatial correlation is lowest during September and October, when MFB is also > 0.4 in part because WRF-Chem simulates high AOD and aerosol nitrate and sulfate concentrations over large regions in eastern North America. The high positive bias in these months is also reflected in the near-surface $PM_{2.5}$ (Fig. S2). A possible explanation for the relatively poor model performance during September and October may derive from the simulation of precipitation. During the majority of calendar months, domain averaged precipitation as simulated by WRF-Chem is slightly positively biased relative to the gridded observational data. However, during September and October, the model exhibits a negative bias (of 8–10 % relative to observations) and substantial underestimation of precipitation in regions of typically high AOD such as the Ohio River valley and along the east coast (Fig. S3).

Empirical quantile-quantile plots of AOD at AERONET stations computed for both simultaneous MODIS observations and WRF-Chem with AERONET observations indicate that the positive bias in WRF-Chem simulated values of AOD is evident across much of the probability distribution (5th to 95th percentile values) at most AERONET stations. However, it is worthy of note that WRF-Chem comparisons with AERONET observations occupy much of the same parameter space as simultaneous MODIS and AERONET observations at those sites (Fig. 6a). Thus, model simulations reproduce the range and probability of low-uncertainty AERONET measured AOD nearly as well as MODIS.

3.2 Evaluation of AE

As described above, AE is retrieved with much lower confidence than AOD from the MODIS measurements. Nevertheless, the correlation between WRF-Chem and MODIS monthly mean AE seems to be independent of season and lies between 0.28

and 0.52 for all months except April, May and November when it is lower, whereas r is always < 0.25 when comparing with MISR (Fig. 5b). As for AOD, we computed the Spearman's rank correlation coefficient to reduce the possible bias due to few outliers and the smaller sample size in MISR data (N varies between 2300–5500 depending on the month and is approximately 5 times smaller than the sample size for MODIS). The AE RMSD relative to MODIS or MISR does not exhibit a clear seasonal pattern and the ratio of spatial standard deviations in the AE fields is always lower than 1, indicating more spatial variability in the satellite retrievals than in WRF-Chem. The degree to which these results are symptomatic of the difficulties in retrieving AE from the remote sensing observations is unclear. When the AE values are treated as binary samples (< 1 indicating coarse mode aerosols dominate, while $AE > 1$ indicating a dominance of the fine mode) and presented as a contingency table, WRF-Chem and MODIS simultaneously identify coarse mode dominance (i.e. $AE < 1$) in 18 % of grid cells (Table 5). After cloud screening, WRF-Chem simulates 31 % of grid cells as exhibiting annual mean $AE > 1$, while MODIS indicates a larger fraction of grid cells with $AE > 1$ (80 %, Table 5). Both WRF-Chem and MODIS indicate the highest prevalence of fine mode particles during the warm months with highest agreement for co-identification (above 50 %) during June–September. Co-identification of coarse mode particles is highest in the winter and spring months (above 20 % during February–May and December, Table 5). However, when a χ^2 test is applied to the frequency of fine and coarse particles identified by WRF-Chem and MODIS, for all months except January and April, the p value is < 0.01 , thus we reject the null hypothesis of equal distribution of fine and coarse mode particles identified by MODIS and WRF-Chem. The two data sets agree on 29 % of the cases when trying to identify fine mode particles and approximately 53 % of the cells are misclassified with MODIS usually identifying a high prevalence of fine aerosols than WRF-Chem. AE from WRF-Chem is also negatively biased relative to AERONET observations, with $MFB = -0.59$ indicating WRF-Chem is simulating a greater prevalence of coarse mode aerosols (Table 3, Figs. 2 and 4b). EQQ plots for all sites show good accord between WRF-Chem and AERONET observations, as in

How skillfully can we simulate drivers of aerosol direct climate forcing at the regional scale?

P. Crippa et al.

Title Page

Abstract

Introduction

Conclusions

References

Tables

Figures

◀

▶

◀

▶

Back

Close

Full Screen / Esc

Printer-friendly Version

Interactive Discussion



5 dicated by the relatively consistent fractional error across the entire range of simulated and observed AE (Fig. 6b). Simulations from previous studies have also shown a systematic negative bias of simulated AE vs. MODIS observations. Highest biases have been noted in regions dominated by dust aerosols or when the model overestimates the dust loading, since aerosol population mean diameter is inversely proportional to AE (Colarco et al., 2014; Balzarini et al., 2014). Sources of the biases in our study, include the simplified treatment of the size distribution, weaknesses in the emission inventory or uncertainties in meteorological variables affecting particle growth (e.g. temperature and relative humidity). Future work will focus on examining these sensitivities.

10 3.3 AOD extremes

Averaged across the entire simulation period, WRF-Chem correctly identifies 70 % of locations with extreme and non-extreme AOD in the MODIS observations (i.e. the Accuracy = 70 %, Table 6). The overall TS and HR also indicate the geographic location of extreme AOD is similar between the model and satellite retrievals. The annual mean HR, which is defined as the proportion of grid cells with extreme AOD co-identified by WRF-Chem and MODIS relative to MODIS extremes, is 41 %. The annual mean TS, which also takes into account false alarms, is 27 % (Table 6).

For each month, the HR is significantly higher than the probability of co-identification of extremes by random chance (i.e. $p_0 = 0.25^2 = 0.0625$), since the test statistic

20 $\frac{HR - p_0^2}{\sqrt{\frac{p_0 \times (1 - p_0)}{N}}}$ is always larger than the critical value at 1 % (i.e. 2.575). HR and TS vary

seasonally, with highest skill during summer months (HR up to 70 % and TS up to 54 %), and lowest skill during winter and early spring (minimum HR = 29 % and minimum TS = 17 %) (Table 6 and Fig. 7). The relatively low skill in identifying the spatial occurrence of high AOD during winter and spring may reflect the relatively low AOD and low spatial variability during this season, which means “extreme” AOD may differ

How skillfully can we simulate drivers of aerosol direct climate forcing at the regional scale?

P. Crippa et al.

Title Page

Abstract

Introduction

Conclusions

References

Tables

Figures

◀

▶

◀

▶

Back

Close

Full Screen / Esc

Printer-friendly Version

Interactive Discussion



only marginally from the “non-extreme” areas (see Fig. S4 for monthly comparisons of extreme area identification).

The spatial distribution of extreme AOD also displays some seasonality with areas of AOD > p75 concentrated over coastal regions and the southern states during summer months and smaller areas during winter and early spring (Fig. 7). Despite the relatively low simultaneous identification of extremes during cold seasons, the location of extremes moves from the coast to the Great Lakes region and Midwest states in both the model and MODIS (see Fig. S3). During winter and spring months WRF-Chem simulates more areas with extreme AOD over coastal regions, whereas MODIS shows more spatial variability and predicts higher AOD in the Great Lakes area and in the states west of Illinois. Conversely, WRF-Chem underestimates areas of extreme AOD relative to MODIS in the northern regions of the domain, possibly due to the underestimation of sulfate-aerosol. These two observations may be explained noting that the mass fraction of aerosol nitrate in the accumulation and coarse mode predicted by WRF-Chem during most of fall and winter months dominates the sulfate fraction over virtually all of the domain (see Fig. S5), whereas point observations indicate aerosol nitrate mass fraction is dominant only over the Central Great Plains (Hand et al., 2012). This may be related to an overestimation of aerosol-nitrate as a result of the impact of air temperature and relative humidity on aerosol ammonium nitrate (NH₄NO₃) stability (Aksoyoglu et al., 2011), as well as an underestimation of aerosol sulfate likely due to underestimation of the rate of SO₂ gaseous and aqueous (missing) oxidation, or underestimation of the nighttime boundary layer height which impacts sulfate formation near the surface (Tuccella et al., 2012). Localized negative biases in the model over the coast may be associated with the higher uncertainties in MODIS retrievals at coastlines.

Extreme AOD exhibits relatively large spatial scales of coherence in both the WRF-Chem simulations and MODIS L2 observations (Fig. 8). Consistent with prior analyses of L3 MODIS data (Sullivan et al., 2015), the largest scales of coherence are found in fall. In all seasons except for winter the probability of co-occurrence of extremes at the domain center and any other grid cell in the simulation domain is > 0.5 up to a distance

How skillfully can we simulate drivers of aerosol direct climate forcing at the regional scale?

P. Crippa et al.

Title Page	
Abstract	Introduction
Conclusions	References
Tables	Figures
◀	▶
◀	▶
Back	Close
Full Screen / Esc	
Printer-friendly Version	
Interactive Discussion	



Lowest model-observations agreement is found in September and October and is at least partially attributable to a dry bias in WRF-Chem (Fig. S3).

- In part because of the difficulties in retrieving robust estimates of AE, few previous studies have evaluated model simulated AE values. We show that AE as simulated by WRF-Chem over eastern North America is negatively biased relative to MODIS (MFB = -0.10) and AERONET (MFB = -0.64). This bias indicates WRF-Chem simulates a larger fraction of coarse mode particles than is evident in the remote sensing observations (see Table 3 and 5). While some of the bias relative to MODIS may reflect high observational uncertainty, the bias relative to AERONET is consistent with prior research (Table 1) and is symptomatic of relatively poor model performance for this metric. Causes of the model error may include insufficiently detailed treatment of size distribution or inaccurate representation of aerosol composition and mixing state which affect the simulated size distribution and thus AE (Li et al., 2015; Curci et al., 2014). Further, weaknesses in the emission inventory (e.g. size resolution of primary emissions), as suggested by the systematic bias in simulated $PM_{2.5}$ concentrations relative to ground-based observations, and/or biases in the representation of meteorological conditions critical to determining aerosol nitrate concentrations may also affect model performance. Currently it is not possible to fully attribute the relative importance of these error sources.
- The majority of prior model evaluation exercises have tended to focus on the central tendency of the AOD probability distribution. However, the climate and health impacts of aerosols are maximized under high aerosol loadings. We demonstrate that WRF-Chem exhibits some skill in capturing the spatial patterns of extreme aerosol loading, especially during summer months. During this season, the Hit Rate for $AOD > p75$ reaches 70 %. Largest biases are found during winter months and near the coastlines where AOD from MODIS also exhibits largest retrieval uncertainty.

How skillfully can we simulate drivers of aerosol direct climate forcing at the regional scale?

P. Crippa et al.

Title Page

Abstract

Introduction

Conclusions

References

Tables

Figures

◀

▶

◀

▶

Back

Close

Full Screen / Esc

Printer-friendly Version

Interactive Discussion



How skillfully can we simulate drivers of aerosol direct climate forcing at the regional scale?

P. Crippa et al.

[Title Page](#)[Abstract](#)[Introduction](#)[Conclusions](#)[References](#)[Tables](#)[Figures](#)[◀](#)[▶](#)[◀](#)[▶](#)[Back](#)[Close](#)[Full Screen / Esc](#)[Printer-friendly Version](#)[Interactive Discussion](#)

- Boylan, J. W. and Russell, A. G.: PM and light extinction model performance metrics, goals, and criteria for three-dimensional air quality models, *Atmos. Environ.*, 40, 4946–4959, doi:10.1016/j.atmosenv.2005.09.087, 2006.
- Castro, C. L., Pielke, R. A., and Leoncini, G.: Dynamical downscaling: assessment of value retained and added using the Regional Atmospheric Modeling System (RAMS), *J. Geophys. Res.*, 110, D05108, doi:10.1029/2004JD004721, 2005.
- Chu, S. H.: PM_{2.5} episodes as observed in the speciation trends network, *Atmos. Environ.*, 38, 5237–5246, doi:10.1016/j.atmosenv.2004.01.055, 2004.
- Colarco, P., da Silva, A., Chin, M., and Diehl, T.: Online simulations of global aerosol distributions in the NASA GEOS-4 model and comparisons to satellite and ground-based aerosol optical depth, *J. Geophys. Res.-Atmos.*, 115, D14207, doi:10.1029/2009jd012820, 2010.
- Colarco, P. R., Kahn, R. A., Remer, L. A., and Levy, R. C.: Impact of satellite viewing-swath width on global and regional aerosol optical thickness statistics and trends, *Atmos. Meas. Tech.*, 7, 2313–2335, doi:10.5194/amt-7-2313-2014, 2014.
- Curci, G., Hogrefe, C., Bianconi, R., Im, U., Balzarini, A., Baró, R., Brunner, D., Forkel, R., Giordano, L., Hirtl, M., Honzak, L., Jiménez-Guerrero, P., Knote, C., Langer, M., Makar, P. A., Pirovano, G., Pérez, J. L., San José, R., Syrakov, D., Tuccella, P., Werhahn, J., Wolke, R., Žabkar, R., Zhang, J., and Galmarini, S.: Uncertainties of simulated aerosol optical properties induced by assumptions on aerosol physical and chemical properties: an AQMEII-2 perspective, *Atmos. Environ.*, 115, 541–552, doi:10.1016/j.atmosenv.2014.09.009, 2014.
- de Meij, A., Pozzer, A., Pringle, K. J., Tost, H., and Lelieveld, J.: EMAC model evaluation and analysis of atmospheric aerosol properties and distribution with a focus on the Mediterranean region, *Atmos. Res.*, 114–115, 38–69, doi:10.1016/j.atmosres.2012.05.014, 2012.
- Drury, E., Jacob, D. J., Spurr, R. J. D., Wang, J., Shinozuka, Y., Anderson, B. E., Clarke, A. D., Dibb, J., McNaughton, C., and Weber, R.: Synthesis of satellite (MODIS), aircraft (ICARTT), and surface (IMPROVE, EPA-AQS, AERONET) aerosol observations over eastern North America to improve MODIS aerosol retrievals and constrain surface aerosol concentrations and sources, *J. Geophys. Res.-Atmos.*, 115, D14204, doi:10.1029/2009jd012629, 2010.
- Emmons, L. K., Walters, S., Hess, P. G., Lamarque, J.-F., Pfister, G. G., Fillmore, D., Granier, C., Guenther, A., Kinnison, D., Laepple, T., Orlando, J., Tie, X., Tyndall, G., Wiedinmyer, C., Baughcum, S. L., and Kloster, S.: Description and evaluation of the Model for Ozone and Related chemical Tracers, version 4 (MOZART-4), *Geosci. Model Dev.*, 3, 43–67, doi:10.5194/gmd-3-43-2010, 2010.

How skillfully can we simulate drivers of aerosol direct climate forcing at the regional scale?

P. Crippa et al.

Title Page

Abstract

Introduction

Conclusions

References

Tables

Figures

◀

▶

◀

▶

Back

Close

Full Screen / Esc

Printer-friendly Version

Interactive Discussion



Fast, J. D., Gustafson, W. I., Easter, R. C., Zaveri, R. A., Barnard, J. C., Chapman, E. G., Grell, G. A., and Peckham, S. E.: Evolution of ozone, particulates, and aerosol direct radiative forcing in the vicinity of Houston using a fully coupled meteorology-chemistry-aerosol model, *J. Geophys. Res.*, 111, D21305, doi:10.1029/2005JD006721, 2006.

5 Ford, B. and Heald, C. L.: Aerosol loading in the Southeastern United States: reconciling surface and satellite observations, *Atmos. Chem. Phys.*, 13, 9269–9283, doi:10.5194/acp-13-9269-2013, 2013.

Giannouli, M., Kalognomou, E.-A., Mellios, G., Moussiopoulos, N., Samaras, Z., and Fiala, J.: Impact of European emission control strategies on urban and local air quality, *Atmos. Environ.*, 45, 4753–4762, doi:10.1016/j.atmosenv.2010.03.016, 2011.

10 Gkikas, A., Houssos, E. E., Hatzianastassiou, N., Papadimas, C. D., and Bartzokas, A.: Synoptic conditions favouring the occurrence of aerosol episodes over the broader Mediterranean basin, *Q. J. Roy. Meteor. Soc.*, 138, 932–949, doi:10.1002/qj.978, 2012.

Grell, G. A., Peckham, S. E., Schmitz, R., McKeen, S. A., Frost, G., Skamarock, W. C., and Eder, B.: Fully coupled “online” chemistry within the WRF model, *Atmos. Environ.*, 39, 6957–6975, doi:10.1016/j.atmosenv.2005.04.027, 2005.

Guenther, A., Zimmerman, P., and Wildermuth, M.: Natural volatile organic compound emission rate estimates for U.S. woodland landscapes, *Atmos. Environ.*, 28, 1197–1210, doi:10.1016/1352-2310(94)90297-6, 1994.

20 Guenther, A. B., Zimmerman, P. R., Harley, P. C., Monson, R. K., and Fall, R.: Isoprene and monoterpene emission rate variability: model evaluations and sensitivity analyses, *J. Geophys. Res.-Atmos.*, 98, 12609–12617, doi:10.1029/93jd00527, 1993.

Hand, J. L., Schichtel, B. A., Pitchford, M., Malm, W. C., and Frank, N. H.: Seasonal composition of remote and urban fine particulate matter in the United States, *J. Geophys. Res.*, 117, D05209, doi:10.1029/2011JD017122, 2012.

25 Holben, B. N., Eck, T. F., Slutsker, I., Tanre, D., Buis, J. P., Setzer, A., Vermote, E., Reagan, J. A., Kaufman, Y. J., Nakajima, T., Lavenu, F., Jankowiak, I., and Smirnov, A.: AERONET – a federated instrument network and data archive for aerosol characterization, *Remote Sens. Environ.*, 66, 1–16, doi:10.1016/s0034-4257(98)00031-5, 1998.

30 Holben, B. N., Tanre, D., Smirnov, A., Eck, T. F., Slutsker, I., Abuhassan, N., Newcomb, W. W., Schafer, J. S., Chatenet, B., Lavenu, F., Kaufman, Y. J., Castle, J. V., Setzer, A., Markham, B., Clark, D., Frouin, R., Halthore, R., Karneli, A., O'Neill, N. T., Pietras, C., Pinker, R. T., Voss, K.,

How skillfully can we simulate drivers of aerosol direct climate forcing at the regional scale?

P. Crippa et al.

Title Page

Abstract

Introduction

Conclusions

References

Tables

Figures

◀

▶

◀

▶

Back

Close

Full Screen / Esc

Printer-friendly Version

Interactive Discussion

- and Zibordi, G.: An emerging ground-based aerosol climatology: aerosol optical depth from AERONET, *J. Geophys. Res.-Atmos.*, 106, 12067–12097, doi:10.1029/2001jd900014, 2001.
- Kahn, R. A., Gaitley, B. J., Martonchik, J. V., Diner, D. J., Crean, K. A., and Holben, B.: Multiangle Imaging Spectroradiometer (MISR) global aerosol optical depth validation based on 2 years of coincident Aerosol Robotic Network (AERONET) observations, *J. Geophys. Res.-Atmos.*, 110, D10s04, doi:10.1029/2004jd004706, 2005.
- Kahn, R. A., Gaitley, B. J., Garay, M. J., Diner, D. J., Eck, T. F., Smirnov, A., and Holben, B. N.: Multiangle Imaging SpectroRadiometer global aerosol product assessment by comparison with the Aerosol Robotic Network, *J. Geophys. Res.-Atmos.*, 115, D23209, doi:10.1029/2010jd014601, 2010.
- Kinne, S., O'Donnel, D., Stier, P., Kloster, S., Zhang, K., Schmidt, H., Rast, S., Giorgetta, M., Eck, T. F., and Stevens, B.: MAC-v1: a new global aerosol climatology for climate studies, *J. Adv. Model. Earth Syst.*, 5, 704–740, doi:10.1002/jame.20035, 2013.
- Kulmala, M., Asmi, A., Lappalainen, H. K., Baltensperger, U., Brenguier, J.-L., Facchini, M. C., Hansson, H.-C., Hov, Ø., O'Dowd, C. D., Pöschl, U., Wiedensohler, A., Boers, R., Boucher, O., de Leeuw, G., Denier van der Gon, H. A. C., Feichter, J., Krejci, R., Laj, P., Lihavainen, H., Lohmann, U., McFiggans, G., Mentel, T., Pilinis, C., Riipinen, I., Schulz, M., Stohl, A., Swietlicki, E., Vignati, E., Alves, C., Amann, M., Ammann, M., Arabas, S., Artaxo, P., Baars, H., Beddows, D. C. S., Bergström, R., Beukes, J. P., Bilde, M., Burkhardt, J. F., Canonaco, F., Clegg, S. L., Coe, H., Crumeyrolle, S., D'Anna, B., Decesari, S., Gilardoni, S., Fischer, M., Fjaeraa, A. M., Fountoukis, C., George, C., Gomes, L., Halloran, P., Hamburger, T., Harrison, R. M., Herrmann, H., Hoffmann, T., Hoose, C., Hu, M., Hyvärinen, A., Hörrak, U., Iinuma, Y., Iversen, T., Josipovic, M., Kanakidou, M., Kiendler-Scharr, A., Kirkevåg, A., Kiss, G., Klimont, Z., Kolmonen, P., Komppula, M., Kristjánsson, J.-E., Laakso, L., Laaksonen, A., Labonnote, L., Lanz, V. A., Lehtinen, K. E. J., Rizzo, L. V., Makkonen, R., Manninen, H. E., McMeeking, G., Merikanto, J., Minikin, A., Mirme, S., Morgan, W. T., Nemitz, E., O'Donnell, D., Panwar, T. S., Pawlowska, H., Petzold, A., Pienaar, J. J., Pio, C., Plass-Duelmer, C., Prévôt, A. S. H., Pryor, S., Reddington, C. L., Roberts, G., Rosenfeld, D., Schwarz, J., Seland, Ø., Sellegri, K., Shen, X. J., Shiraiwa, M., Siebert, H., Sierau, B., Simpson, D., Sun, J. Y., Topping, D., Tunved, P., Vaattovaara, P., Vakkari, V., Veeffkind, J. P., Visschedijk, A., Vuollekoski, H., Vuolo, R., Wehner, B., Wildt, J., Woodward, S., Worsnop, D. R., van Zadelhoff, G.-J., Zardini, A. A., Zhang, K., van Zyl, P. G., Kerminen, V.-M., S Carslaw, K., and Pandis, S. N.: General overview: European Integrated project on Aerosol Cloud Climate

How skillfully can we simulate drivers of aerosol direct climate forcing at the regional scale?

P. Crippa et al.

Title Page

Abstract

Introduction

Conclusions

References

Tables

Figures

◀

▶

◀

▶

Back

Close

Full Screen / Esc

Printer-friendly Version

Interactive Discussion



and Air Quality interactions (EUCAARI) – integrating aerosol research from nano to global scales, Atmos. Chem. Phys., 11, 13061–13143, doi:10.5194/acp-11-13061-2011, 2011.

Kumar, R., Barth, M. C., Pfister, G. G., Naja, M., and Brasseur, G. P.: WRF-Chem simulations of a typical pre-monsoon dust storm in northern India: influences on aerosol optical properties and radiation budget, Atmos. Chem. Phys., 14, 2431–2446, doi:10.5194/acp-14-2431-2014, 2014.

Kurokawa, J., Ohara, T., Morikawa, T., Hanayama, S., Janssens-Maenhout, G., Fukui, T., Kawashima, K., and Akimoto, H.: Emissions of air pollutants and greenhouse gases over Asian regions during 2000–2008: Regional Emission inventory in ASia (REAS) version 2, Atmos. Chem. Phys., 13, 11019–11058, doi:10.5194/acp-13-11019-2013, 2013.

Lee, Y. H., Adams, P. J., and Shindell, D. T.: Evaluation of the global aerosol microphysical ModelE2-TOMAS model against satellite and ground-based observations, Geosci. Model Dev., 8, 631–667, doi:10.5194/gmd-8-631-2015, 2015.

Levy, R. C., Remer, L. A., and Dubovik, O.: Global aerosol optical properties and application to Moderate Resolution Imaging Spectroradiometer aerosol retrieval over land, J. Geophys. Res.-Atmos., 112, 15, doi:10.1029/2006jd007815, 2007.

Levy, R. C., Remer, L. A., Kleidman, R. G., Mattoo, S., Ichoku, C., Kahn, R., and Eck, T. F.: Global evaluation of the Collection 5 MODIS dark-target aerosol products over land, Atmos. Chem. Phys., 10, 10399–10420, doi:10.5194/acp-10-10399-2010, 2010.

Li, S., Kahn, R., Chin, M., Garay, M. J., and Liu, Y.: Improving satellite-retrieved aerosol microphysical properties using GOCART data, Atmos. Meas. Tech., 8, 1157–1171, doi:10.5194/amt-8-1157-2015, 2015.

Matsuura, K. and Willmott, C. J.: Terrestrial precipitation: 1900–2008 gridded monthly time series, available at: http://climate.geog.udel.edu/~climate/html_pages/download.html (last access: July 2015), 2009.

Michou, M., Nabat, P., and Saint-Martin, D.: Development and basic evaluation of a prognostic aerosol scheme (v1) in the CNRM Climate Model CNRM-CM6, Geosci. Model Dev., 8, 501–531, doi:10.5194/gmd-8-501-2015, 2015.

Myhre, G., Samset, B. H., Schulz, M., Balkanski, Y., Bauer, S., Bernsten, T. K., Bian, H., Bellouin, N., Chin, M., Diehl, T., Easter, R. C., Feichter, J., Ghan, S. J., Hauglustaine, D., Iversen, T., Kinne, S., Kirkevåg, A., Lamarque, J.-F., Lin, G., Liu, X., Lund, M. T., Luo, G., Ma, X., van Noije, T., Penner, J. E., Rasch, P. J., Ruiz, A., Seland, Ø., Skeie, R. B., Stier, P., Takemura, T., Tsigaridis, K., Wang, P., Wang, Z., Xu, L., Yu, H., Yu, F., Yoon, J.-H., Zhang, K.,

How skillfully can we simulate drivers of aerosol direct climate forcing at the regional scale?

P. Crippa et al.

Title Page

Abstract

Introduction

Conclusions

References

Tables

Figures

◀

▶

◀

▶

Back

Close

Full Screen / Esc

Printer-friendly Version

Interactive Discussion



Zhang, H., and Zhou, C.: Radiative forcing of the direct aerosol effect from AeroCom Phase II simulations, *Atmos. Chem. Phys.*, 13, 1853–1877, doi:10.5194/acp-13-1853-2013, 2013.

Nabat, P., Somot, S., Mallet, M., Michou, M., Sevault, F., Driouech, F., Meloni, D., di Sarra, A., Di Biagio, C., Formenti, P., Sicard, M., Léon, J.-F., and Bouin, M.-N.: Dust aerosol radiative effects during summer 2012 simulated with a coupled regional aerosol–atmosphere–ocean model over the Mediterranean, *Atmos. Chem. Phys.*, 15, 3303–3326, doi:10.5194/acp-15-3303-2015, 2015.

Nair, V. S., Solmon, F., Giorgi, F., Mariotti, L., Babu, S. S., and Moorthy, K. K.: Simulation of South Asian aerosols for regional climate studies, *J. Geophys. Res.*, 117, D04209, doi:10.1029/2011JD016711, 2012.

Pereira, S. N., Wagner, F., and Silva, A. M.: Seven years of measurements of aerosol scattering properties, near the surface, in the southwestern Iberia Peninsula, *Atmos. Chem. Phys.*, 11, 17–29, doi:10.5194/acp-11-17-2011, 2011.

Pfister, G. G., Parrish, D. D., Worden, H., Emmons, L. K., Edwards, D. P., Wiedinmyer, C., Diskin, G. S., Huey, G., Oltmans, S. J., Thouret, V., Weinheimer, A., and Wisthaler, A.: Characterizing summertime chemical boundary conditions for air masses entering the US West Coast, *Atmos. Chem. Phys.*, 11, 1769–1790, doi:10.5194/acp-11-1769-2011, 2011.

Rea, G., Turquety, S., Menut, L., Briant, R., Mailler, S., and Siour, G.: Source contributions to 2012 summertime aerosols in the Euro-Mediterranean region, *Atmos. Chem. Phys. Discuss.*, 15, 8191–8242, doi:10.5194/acpd-15-8191-2015, 2015.

Remer, L. A., Kaufman, Y. J., Tanre, D., Mattoo, S., Chu, D. A., Martins, J. V., Li, R. R., Ichoku, C., Levy, R. C., Kleidman, R. G., Eck, T. F., Vermote, E., and Holben, B. N.: The MODIS aerosol algorithm, products, and validation, *J. Atmos. Sci.*, 62, 947–973, doi:10.1175/jas3385.1, 2005.

Schell, B., Ackermann, I. J., Hass, H., Binkowski, F. S., and Ebel, A.: Modeling the formation of secondary organic aerosol within a comprehensive air quality model system, *J. Geophys. Res.-Atmos.*, 106, 28275–28293, doi:10.1029/2001jd000384, 2001.

Shepard, D.: A two-dimensional interpolation function for irregularly-spaced data, *Proceedings of the 1968 23rd ACM National Conference*, 1968.

Sič, B., El Amraoui, L., Marécal, V., Josse, B., Arteta, J., Guth, J., Joly, M., and Hamer, P. D.: Modelling of primary aerosols in the chemical transport model MOCAGE: development and evaluation of aerosol physical parameterizations, *Geosci. Model Dev.*, 8, 381–408, doi:10.5194/gmd-8-381-2015, 2015.

How skillfully can we simulate drivers of aerosol direct climate forcing at the regional scale?

P. Crippa et al.

Title Page

Abstract

Introduction

Conclusions

References

Tables

Figures

◀

▶

◀

▶

Back

Close

Full Screen / Esc

Printer-friendly Version

Interactive Discussion



Simpson, D., Guenther, A., Hewitt, C. N., and Steinbrecher, R.: Biogenic emissions in Europe. 1. estimates and uncertainties, *J. Geophys. Res.-Atmos.*, 100, 22875–22890, doi:10.1029/95jd02368, 1995.

Spracklen, D. V., Carslaw, K. S., Merikanto, J., Mann, G. W., Reddington, C. L., Pickering, S., Ogren, J. A., Andrews, E., Baltensperger, U., Weingartner, E., Boy, M., Kulmala, M., Laakso, L., Lihavainen, H., Kivekäs, N., Komppula, M., Mihalopoulos, N., Kouvarakis, G., Jennings, S. G., O'Dowd, C., Birmili, W., Wiedensohler, A., Weller, R., Gras, J., Laj, P., Sellegri, K., Bonn, B., Krejci, R., Laaksonen, A., Hamed, A., Minikin, A., Harrison, R. M., Talbot, R., and Sun, J.: Explaining global surface aerosol number concentrations in terms of primary emissions and particle formation, *Atmos. Chem. Phys.*, 10, 4775–4793, doi:10.5194/acp-10-4775-2010, 2010.

Stocker, T. F., Qin, D., Plattner, G.-K., Alexander, L. V., Allen, S. K., Bindoff, N. L., Breion, F. M., Church, J. A., Cubasch, U., Emori, S., Forster, P., Friedlingstein, P., Gillett, N., Gregory, J. M., Hartmann, D. L., Jansen, E., Kirtman, B., Knutti, R., Krishna Kumar, K., Lemke, P., Marotzke, J., Masson-Delmotte, V., Meehl, G. A., Mokhov, I. I., Piao, S., Ramaswamy, V., Randall, D., Rhein, M., Rojas, M., Sabine, C., Shindell, D., Talley, L. D., Vaughan, D. G., and Xie, S.-P.: Summary for Policymakers, in: *Climate Change 2013: The Physical Science Basis. Contribution of Working Group I to the Fifth Assessment Report of the Intergovernmental Panel on Climate Change*, Cambridge University Press, Cambridge, UK and New York, NY, USA, 33–115, 2013.

Stockwell, W. R., Middleton, P., Chang, J. S., and Tang, X.: The second generation regional acid deposition model chemical mechanism for regional air quality modeling, *J. Geophys. Res.*, 95, 16343–16367, doi:10.1029/JD095iD10p16343, 1990.

Sullivan, R. C., Levy, R. C., and Pryor, S. C.: Spatiotemporal coherence of mean and extreme aerosol particle events over eastern North America as observed from satellite, *Atmos. Environ.*, 112, 126–135, doi:10.1016/j.atmosenv.2015.04.026, 2015.

Taylor, K. E.: Summarizing multiple aspects of model performance in a single diagram, *J. Geophys. Res.-Atmos.*, 106, 7183–7192, doi:10.1029/2000jd900719, 2001.

Tessum, C. W., Hill, J. D., and Marshall, J. D.: Twelve-month, 12 km resolution North American WRF-Chem v3.4 air quality simulation: performance evaluation, *Geosci. Model Dev. Discuss.*, 7, 8433–8476, doi:10.5194/gmdd-7-8433-2014, 2014.

How skillfully can we simulate drivers of aerosol direct climate forcing at the regional scale?

P. Crippa et al.

Title Page

Abstract

Introduction

Conclusions

References

Tables

Figures

◀

▶

◀

▶

Back

Close

Full Screen / Esc

Printer-friendly Version

Interactive Discussion



Tuccella, P., Curci, G., Visconti, G., Bessagnet, B., Menut, L., and Park, R. J.: Modeling of gas and aerosol with WRF/Chem over Europe: evaluation and sensitivity study, *J. Geophys. Res.*, 117, D03303, doi:10.1029/2011JD016302, 2012.

5 Tuccella, P., Curci, G., Grell, G. A., Visconti, G., Crumeroylle, S., Schwarzenboeck, A., and Mensah, A. A.: A new chemistry option in WRF/Chem v. 3.4 for the simulation of direct and indirect aerosol effects using VBS: evaluation against IMPACT-EUCAARI data, *Geosci. Model Dev. Discuss.*, 8, 791–853, doi:10.5194/gmdd-8-791-2015, 2015.

US-EPA: 2005 National Emissions Inventory (NEI), US Environmental Protection Agency available at: ftp://aftp.fsl.noaa.gov/divisions/taq/emissions_data_2005/ (last access: July 2015), 10 2009.

Valenzuela, A., Olmo, F. J., Lyamani, H., Granados-Munoz, M. J., Anton, M., Guerrero-Rascado, J. L., Quirantes, A., Toledano, C., Perez-Ramirez, D., and Alados-Arboledas, L.: Aerosol transport over the western Mediterranean basin: evidence of the contribution of fine particles to desert dust plumes over Alboran Island, *J. Geophys. Res.-Atmos.*, 119, 14028–14044, doi:10.1002/2014jd022044, 2014.

15 Willmott, C. J., Rowe, C. M., and Philpot, W. D.: Small-scale climate maps: a sensitivity analysis of some common assumptions associated with grid-point interpolation and contouring, *Am. Cartographer*, 12, 5–16, doi:10.1559/152304085783914686, 1985.

Wu, S., Mickley, L. J., Kaplan, J. O., and Jacob, D. J.: Impacts of changes in land use and land cover on atmospheric chemistry and air quality over the 21st century, *Atmos. Chem. Phys.*, 20 12, 1597–1609, doi:10.5194/acp-12-1597-2012, 2012.

Xing, J., Mathur, R., Pleim, J., Hogrefe, C., Gan, C.-M., Wong, D. C., Wei, C., Gilliam, R., and Pouliot, G.: Observations and modeling of air quality trends over 1990–2010 across the Northern Hemisphere: China, the United States and Europe, *Atmos. Chem. Phys.*, 15, 25 2723–2747, doi:10.5194/acp-15-2723-2015, 2015.

Zhang, Y., Chen, Y., Sarwar, G., and Schere, K.: Impact of gas-phase mechanisms on Weather Research Forecasting Model with Chemistry (WRF/Chem) predictions: mechanism implementation and comparative evaluation, *J. Geophys. Res.-Atmos.*, 117, D01301, doi:10.1029/2011jd015775, 2012.

How skillfully can we simulate drivers of aerosol direct climate forcing at the regional scale?

P. Crippa et al.

Table 1. Synthesis of some recent prior studies comparing simulated aerosol optical properties from global or regional model simulations with remote sensing products. The first column summarizes the model used, the second the domain and the time period simulated and the third shows the model resolution and summarizes the description of the aerosol size distribution. Columns 4 to 9 summarize the evaluation statistics in terms of the overall correlation coefficient (R), bias (as described using the mean fractional error (MFE)) and root mean square error (RMSE) or mean absolute error (MAE) relative to satellite or AERONET observations as reported in the references shown in column 10.

Model	Domain, Time	Resolution, Aerosol Approach	R AOD vs. Satellite	bias AOD vs. Satellite	R AOD vs. AERONET	bias AOD vs. AERONET	R AE vs. AERONET	RMSE, MAE AE vs. AERONET	Ref
TOMAS in GISS	Global, 2000–2003	$2^\circ \times 2.5^\circ$, Sectional: 15 bins from 3 nm–10 μm	0.63 (average of monthly from 2004–2006, MODIS), 0.73 (average of monthly from 2004–2006, MISR)	MFE: –29% (average of monthly from 2004–2006, MODIS), –34% (average of monthly from 2004–2006, MISR)	–0.7–0.99 (monthly, 28)	–77–72% (monthly, 28)	N/A	N/A	Lee et al. (2015)
GOCART with GEOS DAS	CONUS, 2006–2009	$1^\circ \times 1.25^\circ$, not specified	N/A	N/A	0.5 (2 h average at MISR overpass, 32)	N/A	0.43 (2 h average at MISR overpass, 32)	N/A	Li et al. (2015)
GEMS/MACC aerosol module in CNRM-GAME and CERFACS	Global, 1993–2012	1.4° , Sectional, 12 bins	N/A	Mean relative bias –41–(–52)% (monthly, MISR)	< 0–0.9 (monthly, 166)	N/A	N/A	N/A	Michou et al. (2015)
CNRM-RC5M5	Mediter., Summer 2012	50 km, Sectional, 12 bins	0.64 (seasonal, MODIS), 0.77 (seasonal, MISR), 0.65 (seasonal SEVIRI)	N/A	0.7 (daily, 30)	RMSE ~ 1.75 (daily, 30)	N/A	N/A	Nabat et al. (2015)
CHIMERE chemical transport model with WRF meteorology	Europe, Mediter. –10–40° E, 30–55° N, Summer 2012	50 km, Sectional: 5 bins 40 nm–40 μm	0.35–0.75 (hourly, MODIS)	RMSE: 0.04–0.1 (hourly, MODIS)	0.44–0.73 (hourly, 65)	RMSE: 0.8–0.11 (hourly, 65)	N/A	N/A	Rea et al. (2015)

Title Page

Abstract

Introduction

Conclusions

References

Tables

Figures

◀

▶

◀

▶

Back

Close

Full Screen / Esc

Printer-friendly Version

Interactive Discussion

How skillfully can we simulate drivers of aerosol direct climate forcing at the regional scale?

P. Crippa et al.

Table 1. Continued.

Model	Domain, Time	Resolution, Aerosol Approach	R AOD vs. Satellite	bias AOD vs. Satellite	R AOD vs. AERONET	bias AOD vs. AERONET	R AE vs. AERONET	RMSE, MAE AE vs. AERONET	Ref
MOCAGE	Global, 2007	2° × 2°, Sectional: 6 bins per species	0.322 (daily MODIS)	normalized mean bias 0.098 (daily MODIS)	N/A	N/A	N/A	N/A	Sič et al. (2015)
WRF-Chem	0°–10° E, 50°–55° N; –10°–15° E, 46°–57° N; –15–30° E, 36–62° N, 14–30 May 2008	nested 2–30 km, modal	N/A	0.38 ± 0.12 and 0.42 ± 0.10 domain average AOD from MODIS and model respectively	N/A	N/A	N/A	N/A	Tuccella et al. (2015)
GOCART in GEOS	Global, 2000–2006	1° × 1.25°, dust (8 bins 0.1–10 μm), sea salt (5 bins 0.03–10 μm), carbonaceous/sulfate (modal)	0.747, 0.72 E.US (monthly, MODIS)	N/A	0.707 (monthly, 53)	rms: 0.133 (monthly, 53)	0.81 (monthly, 53)	rms: 0.285 (monthly, 53)	Colarco et al. (2010)
EMAC	Global, Year 2006	1.1° × 1.1°, modal	N/A	Negative (North America)	0.27–0.60 (North America)	RMSE = 0.1–0.2	> 0.5 (Europe)	N/A	de Meij et al. (2012)
GEOS-Chem	N. America, 6 Jul–14 Aug 2004	2° × 2.5°, modal	N/A	N/A	0.87 (study period mean, 24)	N/A	N/A	N/A	Drury et al. (2010)
WRF-Chem	Europe and N. Africa, Year 2010	23 km, Modal and sectional (4 bins: 0.04–10 μm)	N/A	N/A	0.52 (mod) 0.51 (sect)	NMB = –0.06 (mod) NMB = –0.21 (sect) (daily, 12 stations)	N/A	N/A	Balzarini et al. (2014)
RegCM4	South Asia, 2005–2007	50 km, Sectional (4 bins: 0.01–20 μm)	N/A	N/A	0.47–0.71 Monthly, 6	N/A	N/A	N/A	Nair et al. (2012)

Title Page

Abstract Introduction

Conclusions References

Tables Figures

◀ ▶

◀ ▶

Back Close

Full Screen / Esc

Printer-friendly Version

Interactive Discussion



How skillfully can we simulate drivers of aerosol direct climate forcing at the regional scale?

P. Crippa et al.

Title Page

Abstract

Introduction

Conclusions

References

Tables

Figures

◀

▶

◀

▶

Back

Close

Full Screen / Esc

Printer-friendly Version

Interactive Discussion

Table 2. Physical and chemical schemes adopted in the WRF-Chem simulations presented herein.

Simulation settings	Values
Domain size	300 × 300 cells
Horizontal resolution	12 km
Vertical resolution	32 levels up to 50 hPa
Timestep for physics	72 s
Timestep for chemistry	5 s
Physics option	Adopted scheme
Microphysics	WRF Single-Moment 5-class
Longwave Radiation	Rapid Radiative Transfer Model (RRTM)
Shortwave Radiation	Goddard
Surface layer	Monin Obhukov similarity
Land Surface	Noah Land Surface Model
Planetary boundary layer	Mellor–Yamada–Janjich
Cumulus parameterizations	Grell 3
Chemistry option	Adopted scheme
Photolysis	Fast J
Gas-phase chemistry	RADM2
Aerosols	MADE/SORGAM
Anthropogenic emissions	NEI (2005)
Biogenic emissions	Guenther, from USGS land use classification

How skillfully can we simulate drivers of aerosol direct climate forcing at the regional scale?

P. Crippa et al.

Title Page

Abstract

Introduction

Conclusions

References

Tables

Figures

◀

▶

◀

▶

Back

Close

Full Screen / Esc

Printer-friendly Version

Interactive Discussion

Table 3. Spatial Mean Fractional Bias (MFB) over the entire year. Recall $MFB = \frac{1}{N} \sum_1^N \frac{C_m - C_0}{\frac{C_m + C_0}{2}}$, where C_m is the monthly mean AOD or AE simulated by WRF-Chem at a specific location and C_0 refers to the same quantity from MODIS/MISR/AERONET. Thus a negative value indicates the model is negatively biased relative to the observations. The total sample size N is 358 048 and 359 633 when comparing WRF-Chem with MODIS onboard Terra and Aqua respectively. The mean domain averaged AOD and AE from WRF-Chem (after applying the cloud screen) are 0.222 and 1.089, respectively.

Comparisons	MFB AOD	MFB AE
WRF-MODIS (Terra)	0.20	−0.09
WRF-MODIS (Aqua)	0.14	−0.11
WRF-MISR (Terra)	0.16	−0.11
WRF-AERONET	0.50	−0.59
MODIS (Terra)-AERONET	−1.23	−0.13

How skillfully can we simulate drivers of aerosol direct climate forcing at the regional scale?

P. Crippa et al.

Title Page

Abstract

Introduction

Conclusions

References

Tables

Figures

◀

▶

◀

▶

Back

Close

Full Screen / Esc

Printer-friendly Version

Interactive Discussion

Table 4. Contingency table used to compare the fraction of grid cells classified as fine ($AE > 1$) and coarse ($AE < 1$) by MODIS and WRF-Chem.

		MODIS	
		Fine	Coarse
WRF-Chem	Fine	WF/MF	WF/MC
	Coarse	WC/MF	WC/MC

How skillfully can we simulate drivers of aerosol direct climate forcing at the regional scale?

P. Crippa et al.

Title Page

Abstract

Introduction

Conclusions

References

Tables

Figures

◀

▶

◀

▶

Back

Close

Full Screen / Esc

Printer-friendly Version

Interactive Discussion



Table 5. Contingency table showing the fraction of grid cells simultaneously identified as fine (WF/MF) or coarse (WC/MC) mode particles by WRF-Chem and MODIS, as well as cells with different classification (columns 4 and 5). Recall a threshold of $AE = 1$ is used to define fine ($AE > 1$) and coarse mode ($AE < 1$) dominance. Months in bold indicate the distribution of observed and simulated fine/coarse mode fractions are significantly different (p value < 0.01) according to the χ^2 test described in Sect. 2.3.

Month	WF/MF	WC/MC	WF/MC	WC/MF
1	0.025	0.176	0.007	0.792
2	0.030	0.241	0.004	0.725
3	0.005	0.297	0.001	0.697
4	0.013	0.230	0.004	0.753
5	0.141	0.204	0.028	0.628
6	0.541	0.122	0.055	0.283
7	0.623	0.094	0.030	0.252
8	0.520	0.061	0.017	0.402
9	0.561	0.118	0.032	0.288
10	0.486	0.145	0.088	0.281
11	0.321	0.179	0.058	0.442
12	0.164	0.248	0.015	0.573
Mean	0.286	0.176	0.028	0.510

How skillfully can we simulate drivers of aerosol direct climate forcing at the regional scale?

P. Crippa et al.

Table 6. Synthesis of the skill with which WRF-Chem identifies the spatial distribution and location of extreme AOD values. Cells with extreme AOD are identified as exceeding the 75th percentile computed on a monthly basis across space from monthly averaged daily means. The second column reports the Accuracy, which indicates the spatial coherence of extremes and non-extremes between WRF-Chem and MODIS. The Accuracy metric is computed as the sum of cells co-identified as exceeding the 75th percentile and not exceeding that threshold by WRF-Chem and MODIS (Terra) relative to the total number of cells with valid data (fifth column, N). The third column reports the Threat Score (TS) which indicates the probability of correctly forecasting extreme AOD conditional upon either forecasting or observing extremes. The fourth column shows the Hit Rate (HR) (i.e. probability of correct forecast), which is the proportion of cells correctly identified as extremes by WRF-Chem relative to MODIS extremes. Values in parenthesis refer to the same metrics when comparing WRF-Chem and MODIS onboard the Aqua satellite.

Month	Accuracy	TS	HR	N
Jan	0.664 (0.651)	0.196 (0.178)	0.328 (0.302)	14 899 (15 051)
Feb	0.654 (0.583)	0.182 (0.091)	0.308 (0.167)	13 721 (13 643)
Mar	0.656 (0.647)	0.185 (0.173)	0.312 (0.295)	16 641 (16 541)
Apr	0.645 (0.680)	0.169 (0.219)	0.289 (0.360)	25 265 (24 974)
May	0.664 (0.699)	0.196 (0.248)	0.327 (0.397)	32 770 (31 239)
Jun	0.796 (0.800)	0.420 (0.428)	0.592 (0.600)	36 148 (34 654)
Jul	0.850 (0.823)	0.538 (0.477)	0.700 (0.646)	36 055 (35 480)
Aug	0.834 (0.832)	0.500 (0.496)	0.667 (0.663)	39 173 (39 130)
Sep	0.667 (0.665)	0.200 (0.197)	0.333 (0.329)	35 883 (35 081)
Oct	0.656 (0.665)	0.185 (0.198)	0.311 (0.330)	29 662 (26 456)
Nov	0.703 (0.696)	0.254 (0.245)	0.405 (0.393)	21 630 (19 538)
Dec	0.648 (0.653)	0.173 (0.181)	0.295 (0.306)	14 914 (14 527)
Mean	0.703 (0.699)	0.266 (0.261)	0.406 (0.399)	26 397 (25 526)

[Title Page](#)
[Abstract](#)
[Introduction](#)
[Conclusions](#)
[References](#)
[Tables](#)
[Figures](#)
[◀](#)
[▶](#)
[◀](#)
[▶](#)
[Back](#)
[Close](#)
[Full Screen / Esc](#)
[Printer-friendly Version](#)
[Interactive Discussion](#)


How skillfully can we simulate drivers of aerosol direct climate forcing at the regional scale?

P. Crippa et al.

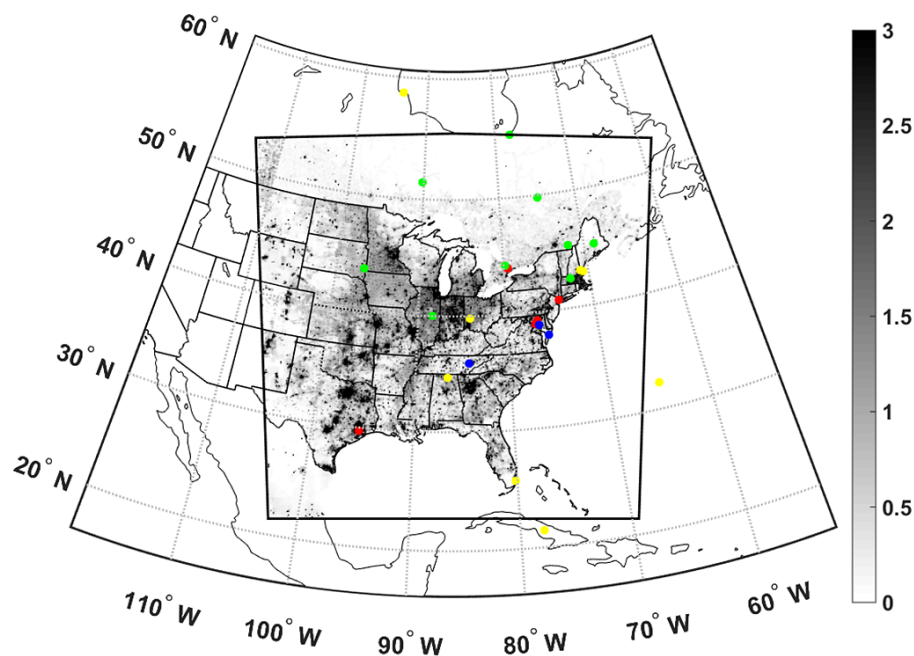


Figure 1. Location of the AERONET stations (colored dots) used in this study and mean daily PM_{2.5} emissions [$\text{mgm}^{-2} \text{day}^{-1}$] during 2008 (gray shading). Colors indicate the AERONET site classification based on (Kinne et al., 2013): polluted (red), land (green), coastal (blue), un-classified (yellow).

How skillfully can we simulate drivers of aerosol direct climate forcing at the regional scale?

P. Crippa et al.

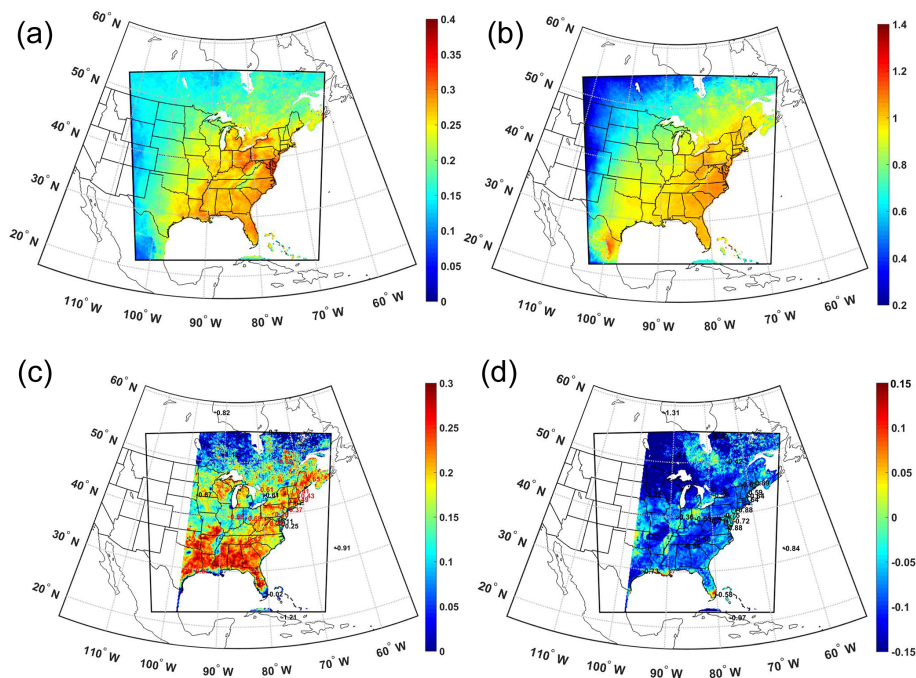


Figure 2. Mean (a) AOD and (b) AE simulated by WRF-Chem during the year 2008. The mean values are computed after applying a cloud mask. Mean Fractional Bias (MFB) for (c) AOD and (d) AE for WRF-Chem relative to MODIS (Terra) (similar results are found for Aqua). The numbers in panels c-d are MFB for WRF-Chem vs. AERONET stations (red numbers indicate WRF-Chem vs. AERONET has a larger MFB than WRF-Chem vs. MODIS whereas black numbers indicate a lower bias in the comparison with AERONET). The inner black frame indicates the entire model domain, while as stated in the text model evaluation is only undertaken for longitudes east of 98° W.

Title Page

Abstract

Introduction

Conclusions

References

Tables

Figures

◀

▶

◀

▶

Back

Close

Full Screen / Esc

Printer-friendly Version

Interactive Discussion

How skillfully can we simulate drivers of aerosol direct climate forcing at the regional scale?

P. Crippa et al.

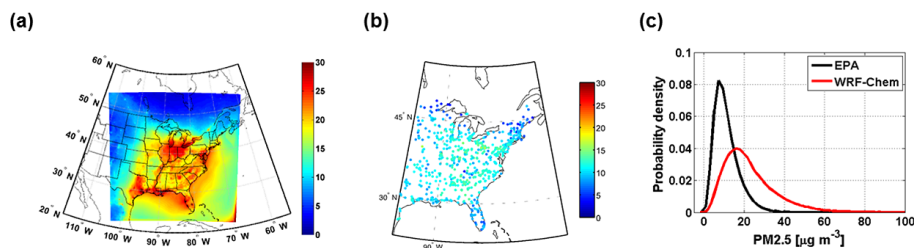


Figure 3. Mean daily PM_{2.5} concentrations [$\mu\text{g m}^{-3}$] during 2008 as **(a)** simulated by WRF-Chem in the layer closest to the surface and **(b)** observed at 1230 EPA sites. Panel **(c)** shows the probability distribution of daily mean PM_{2.5} concentrations observed (black line) and simulated (red line) at the measurement stations.

Title Page

Abstract

Introduction

Conclusions

References

Tables

Figures

◀

▶

◀

▶

Back

Close

Full Screen / Esc

Printer-friendly Version

Interactive Discussion

How skillfully can we simulate drivers of aerosol direct climate forcing at the regional scale?

P. Crippa et al.

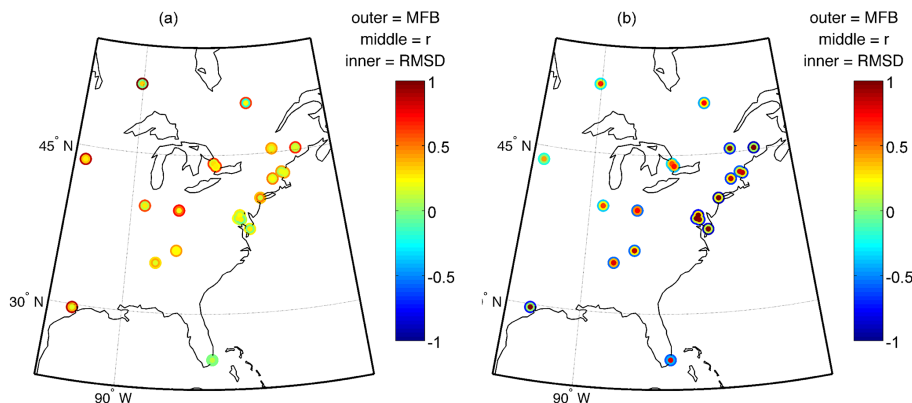


Figure 4. Summary statistics of comparisons of WRF-Chem simulations of **(a)** AOD and **(b)** AE relative to simultaneous observations at the AERONET sites. The symbols at each AERONET station report MFB (outer circle), correlation coefficient (r) (middle) and root mean squared difference (RMSD) (inner). Note: for a location to be included in this analysis at least 20 coincident observations and simulations must be available.

Title Page

Abstract

Introduction

Conclusions

References

Tables

Figures

◀

▶

◀

▶

Back

Close

Full Screen / Esc

Printer-friendly Version

Interactive Discussion

How skillfully can we simulate drivers of aerosol direct climate forcing at the regional scale?

P. Crippa et al.

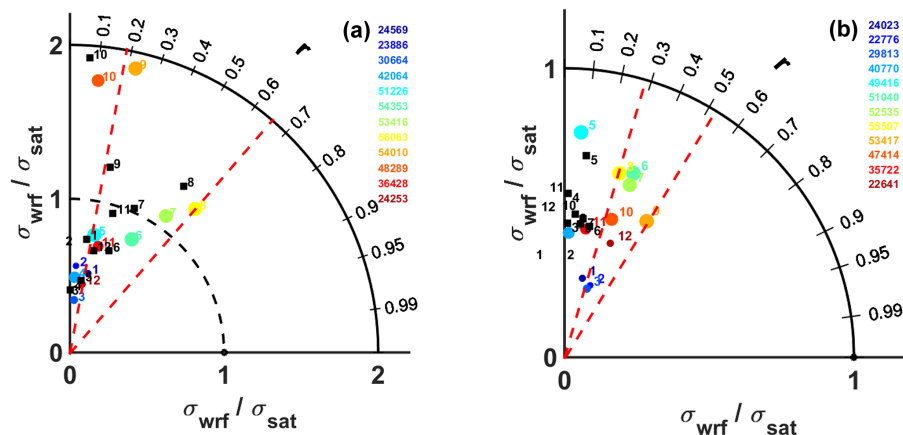


Figure 5. Taylor diagrams comparing the spatial fields of monthly mean **(a)** AOD and **(b)** AE from WRF-Chem vs. MODIS-Terra (color dots) or MISR (black squares). The numbers shown in the frames denote the month (e.g. 1 = January). The numbers shown in the legend indicate the sample size of WRF-Chem data used for computing the monthly mean and the scale of the dots is proportional to the sample size. Note the change in scale for the ratio of standard deviations between the frames. The red dashed lines define the sector with Spearman's rank correlation coefficient between **(a)** 0.18–0.66 for AOD and **(b)** 0.28–0.52 for AE which comprise at least two thirds of the months. Each dot/square summarizes the statistics (i.e. RMSD, ratio of standard deviations and correlation coefficient) of the WRF-Chem vs. MODIS/MISR comparison for a single month.

How skillfully can we simulate drivers of aerosol direct climate forcing at the regional scale?

P. Crippa et al.

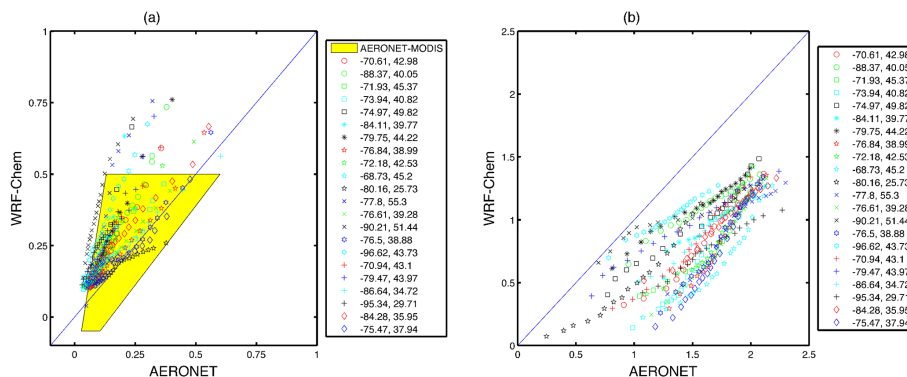


Figure 6. Empirical quantile-quantile (EQQ) plots of **(a)** AOD and **(b)** AE of the 5th to 95th percentile as simulated by WRF-Chem relative to 22 AERONET stations (their longitude (E) and latitude (N) is reported in the legend). The yellow shading shows the data envelope for EQQ plots of AERONET and MODIS. For inclusion in the analysis a location must have at least 20 coincident observations and simulations in the grid cell containing the AERONET station. Note MODIS uncertainty in the retrievals (± 0.05) in near zero AOD conditions may lead to negative AOD values which are considered valid. The parameter space for MODIS-AERONET comparisons of AE are not shown because AE from the MODIS L2 data product are strongly bimodal (see examples given in Fig. 1 in the Supplement).

Title Page

Abstract

Introduction

Conclusions

References

Tables

Figures

◀

▶

◀

▶

Back

Close

Full Screen / Esc

Printer-friendly Version

Interactive Discussion

How skillfully can we simulate drivers of aerosol direct climate forcing at the regional scale?

P. Crippa et al.

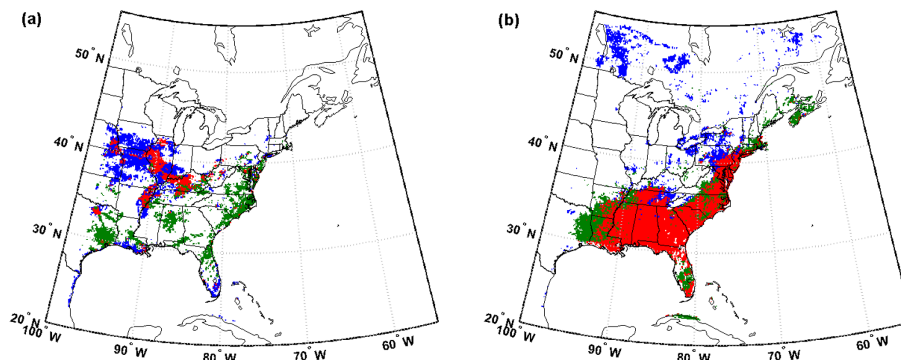


Figure 7. Spatial coherence in extreme AOD (i.e. the occurrence of AOD above the 75th percentile value) from WRF-Chem and MODIS Terra during **(a)** March (03/2008) and **(b)** July (07/2008). Green areas denote grid cells defined as experiencing extreme AOD only in the WRF-Chem simulations, blue pixels indicate extreme values as diagnosed using MODIS, while red pixels indicate areas where the occurrence of extreme values is indicated by both the WRF-Chem simulations and the MODIS observations.

[Title Page](#)[Abstract](#)[Introduction](#)[Conclusions](#)[References](#)[Tables](#)[Figures](#)[◀](#)[▶](#)[◀](#)[▶](#)[Back](#)[Close](#)[Full Screen / Esc](#)[Printer-friendly Version](#)[Interactive Discussion](#)

How skillfully can we simulate drivers of aerosol direct climate forcing at the regional scale?

P. Crippa et al.

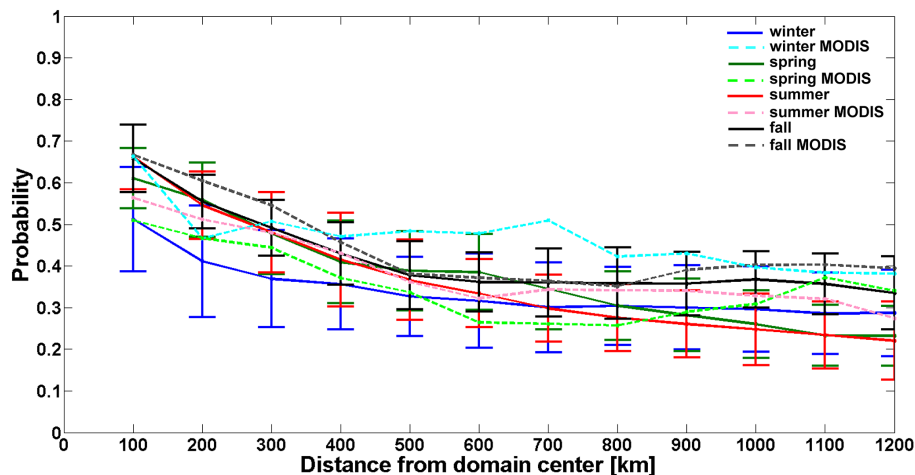


Figure 8. Mean and error bars (± 1 standard deviation from the mean) of the probability of co-occurrence of extreme AOD (i.e. AOD > 75th percentile) at the reference location (i.e. domain center) and any other simulated grid cell during different seasons. The distance between the reference point and each grid cell centroid was binned using 100 km distance classes. Solid lines indicate mean seasonal spatial scales simulated by WRF-Chem, whereas dashed lines are observed means from L2 MODIS data (only the mean of the coherence ratios is plotted for the MODIS data).

[Title Page](#)
[Abstract](#)
[Introduction](#)
[Conclusions](#)
[References](#)
[Tables](#)
[Figures](#)
[◀](#)
[▶](#)
[◀](#)
[▶](#)
[Back](#)
[Close](#)
[Full Screen / Esc](#)
[Printer-friendly Version](#)
[Interactive Discussion](#)
